CHEMISTRY
A EUROPEAN JOURNAL

DOI: 10.1002/chem.200902820

Reversible P_4 Activation with Nickel(I) and an η^3-Coordinated Tetraphosphorus Ligand between Two Ni^I Centers

Shenglai Yao,[a] Yun Xiong,[a] Carsten Milsmann,[b] Eckhard Bill,[b] Stefan Pfirrmann,[c] Christian Limberg,[c] and Matthias Driess*[a]

Dedicated to Professor Martin Jansen on the occasion of his 65th birthday

The direct activation of small molecules such as H_2, O_2, N_2, and P_4 has received considerable attention because of their key role in preparing value-added products. Owing to the growing commercial interest in organophosphorus compounds and environmental protection, P_4 activation requires far more facile methods for benign processes. Commonly, P_4 can be activated by transition metals and exhibits an intriguingly rich coordination ability to the latter.[1–3] Accordingly, several transition-metal complexes bearing a η^1- or η^2-P_4 ligand have been described and crystallographically characterized (**A**–**C**, Scheme 1) since the first transition-metal complex $[(PPh_3)_2ClRh(\eta^2\text{-}P_4)]$ was prepared.[2] Even complexes with a η^4-tetraphosphorus ligand (**D**) have been synthesized and characterized, but no η^3-coordinated P_4 species (**E**) has been reported to date.[1]

Reports on the activation of white phosphorus by main group complexes are relatively rare.[4–6,7b] Striking examples comprise the reactions of some alkaline metal organometallic and low-oxidation-state Group 13 complexes with P_4.[4] Over the last few years, the utilization of N-heterocyclic carbenes (NHCs) and carbene-analogues such as a N-heterocyclic silylene has received particular attention in the area of nonmetal-mediated P_4 activation.[5,6,7]

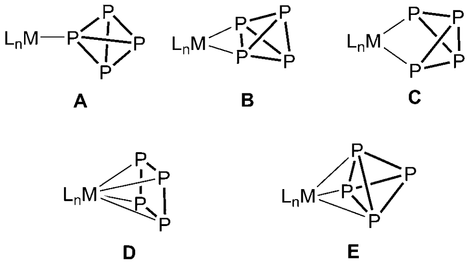

Scheme 1. Various coordination types of P_4 to metal centers.

Recently we have demonstrated that the utilization of the β-diketiminate nickel(I) complex $[(L^{iPr}Ni)_2\cdot toluene]$[8] ($L^{iPr}$ = $CH[CMeN(2,6\text{-}iPr_2C_6H_3)]_2$) leads to the facile activation of O_2, S_8, and elemental selenium and tellurium, yielding the superchalcogenide complexes $L^{iPr}NiO_2$[9a] and $L^{iPr}NiS_2$,[9b] as well as the butterfly-like complexes $[(L^{iPr}Ni)_2E_2]$ (E = S, Se, and Te),[9b,c] respectively. Intriguingly, the $L^{iPr}Ni^I$ moiety is even capable of activating N_2, giving dinitrogen complexes with a $[Ni(\mu\text{-}\eta^1\text{:}\eta^1\text{-}N_2)Ni]$ core.[9d,e] The remarkable reactivity of the Ni^I complexes prompted us to probe whether they can also be employed to activate P_4. Herein we report on the unusual activation of white phosphorus with β-diketiminate nickel(I) complexes, which leads to the remarkable dinuclear nickel complexes $[(L^{iPr}Ni)_2P_4]$ (**1a**) and $[(L^{Et}Ni)_2P_4]$ (**1b**; L^{Et} = $CH[CMeN(2,6\text{-}Et_2C_6H_3)]_2$), featuring a doubly η^3-coordinated P_4 moiety (Scheme 2). Remarkably, the P–P bond activation occurs without reduction of the P_4 ligand to formally P_4^{2-} by Ni^I and can be reversible.

Activation of white phosphorus by the β-diketiminate nickel(I) toluene complex $[(L^{iPr}Ni^I)_2\cdot toluene]$[8] has been performed in toluene at −78 °C, which immediately led to a color change of the solution from red to deep green. The completion of the reaction could be ensured by warming up the mixture to room temperature. Subsequently, changing

---

[a] Dr. S. Yao, Dr. Y. Xiong, Prof. Dr. M. Driess
Institute of Chemistry
Metalorganics and Inorganic Materials, Sekr. C2
Technische Universität Berlin
Strasse des 17. Juni 135, 10623 Berlin (Germany)
Fax: (+49) 30-314-29732
E-mail: matthias.driess@tu-berlin.de

[b] Dr. C. Milsmann, Dr. E. Bill
Max-Planck-Institut für Bioanorganische Chemie
Stiftsstrasse 34-36, 45470 Mülheim/Ruhr (Germany)

[c] Dipl.-Chem. S. Pfirrmann, Prof. Dr. C. Limberg
Humboldt-Universität zu Berlin, Institut für Chemie
Brook-Taylor-Strasse 2. 12489 Berlin (Germany)

Supporting information for this article is available on the WWW under http://dx.doi.org/10.1002/chem.200902820.

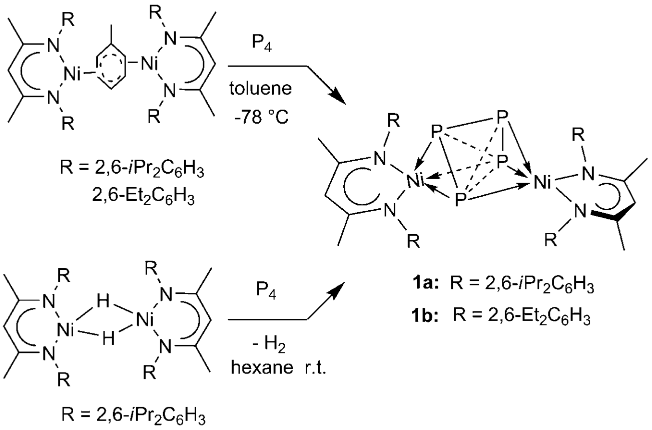

Scheme 2. Synthesis of **1a** and **1b** from white phosphorus.

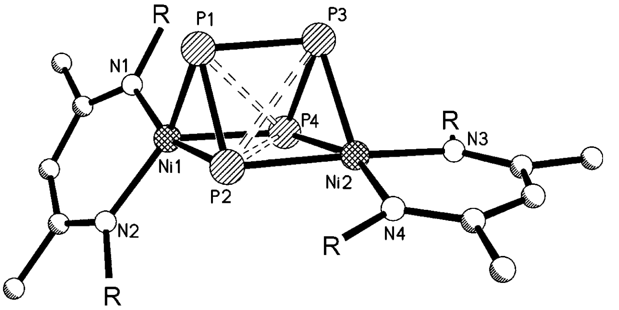

Figure 1. Molecular structure of **1a** ($R=2,6\text{-}i\mathrm{Pr}_2\mathrm{C}_6\mathrm{H}_3$) and **1b** ($R=2,6\text{-}\mathrm{Et}_2\mathrm{C}_6\mathrm{H}_3$). Hydrogen atoms and substituents R are omitted for clarity. Selected distances [Å] and angles [°]: **1a**: P1–P2 2.186(1), P1–P3 2.183(2), P1–P4 2.769(2), P2–P4 2.531(2), P3–P4 2.186(1), P2–P3 2.769(2), Ni1–P4 2.217(1), Ni1–P1 2.195(1), Ni1–P2 2.339(1), Ni2–P2 2.217(1), Ni2–P3 2.195(1), Ni2–P4 2.239(1), Ni1–N1 1.947(3), Ni1–N2 1.968(3), Ni2–N4 1.947(3), Ni2–N3 1.968(3); N1-Ni1-N2 95.0(1). **1b**: P1–P2 2.197(1), P1–P3 2.187(1), P1–P4 2.681(1), P2–P3 2.956(2), P2–P4 2.506(1), P3–P4 2.101(2), Ni1–P4 2.167(1), Ni1–P1 2.203(1), Ni1–P2 2.3285(9), Ni2–P2 2.2535(9), Ni2–P3 2.2576(9), Ni2–P4 2.2693(9), Ni1–N1 1.928(2), Ni1–N2 1.932(2), Ni2–N4 1.937(2), Ni2–N3 1.956(3); N1-Ni1-N2 96.5(1), N4-Ni2-N3 94.8(1).

the solvent to hexane and cooling the concentrated solution to −20 °C afforded **1a** in the form of dark green crystals in 88 % yield (Scheme 2).

Alternatively, **1a** can be prepared from $[(\mathrm{L}^{i\mathrm{Pr}}\mathrm{NiH})_2]$[10] and P_4 in hexane at room temperature under release of dihydrogen. According to EI mass spectrometry (molecular ion *m/z* 1077) and elemental analysis, compound **1a** is a 2:1 adduct of $[\mathrm{L}^{i\mathrm{Pr}}\mathrm{Ni}]$ and P_4 (see the Supporting Information). To examine the influence of steric congestion around the nickel center on the progress of the P_4 activation, we also prepared and employed the less bulky substituted $[(\mathrm{L}^{\mathrm{Et}}\mathrm{Ni})_2\cdot\text{toluene}]$.[11] Similar to the synthesis of **1a**, the latter Ni^{I} precursor affords the analogous $[(\mathrm{L}^{\mathrm{Et}}\mathrm{Ni})_2\mathrm{P}_4]$ complex **1b**, which can be isolated in 84 % yield and has been fully characterized (see the Supporting Information). Compound **1a** crystallizes in toluene in the tetragonal space group $I\bar{4}2d$ and consists of a $\mathrm{Ni}_2\mathrm{P}_4$ prismane-like core featuring two almost planar β-diketiminato Ni subunits twisted away from each other (Figure 1, see the Supporting Information for details). Each nickel center is coordinated by three phosphorus atoms of the P_4 ligand, which leads to significant changes of the P–P distances and thus bond activation. In fact, the complex represents the first complex known to have a η^3-coordinated P_4 ligand (type **E**, Scheme 1). It should be mentioned here that a related $\mathrm{Ni}_2\mathrm{P}_4$ skeleton was observed in $[\{(\eta^5\text{-}\mathrm{C}_5\mathrm{Me}_5)\mathrm{Ni}\}_2\mathrm{P}_4\{(\mathrm{Cr(CO)}_5\}_2]$ with the P_4 moiety coordinated to both the nickel and the chromium atoms.[1e] The P1–P2 (2.186(1) Å), P1–P3 (2.183(2) Å), and P3–P4 (2.186(1) Å) bond lengths are slightly shorter than those in "free" P_4 (2.21 Å). In contrast, the P2–P3 (2.769(2) Å), P2–P4 (2.531(2) Å), and P1–P4 (2.769(2) Å) interatomic distances are much longer than a normal P–P single bond but substantially smaller than the sum of the van der Waals radii (374 pm). The concomitant P–P bond shortening and elongation within the P_4 ligand is reminiscent of the situation in η^2-coordinated P_4 complexes.[12] Complex **1b** crystallizes from diethyl ether in the triclinic space group $P\bar{1}$ and possesses a molecular structure with metric parameters similar to those of **1a** (Figure 1). The Ni–N and Ni–P distances in **1b** are shorter than those in **1a**, apparently due to the smaller steric congestion in **1b** (Ni–N: 1.928(2)–1.956(3) vs. 1.947(3)–1.968(3) Å, and Ni–P: 2.167(1)–2.3285(9) vs. 2.217(1)– 2.339(1) Å). Accordingly, the distance between the nickel centers in **1b** (3.748 Å) is smaller than that in **1a** (3.790 Å). The metric features of the $\mathrm{Ni}_2\mathrm{P}_4$ core in **1a** and **1b** are similar to that of $[\{(\eta^5\text{-}\mathrm{C}_5\mathrm{Me}_5)\mathrm{Ni}\}_2\mathrm{P}_4]$,[1d] which, however, is electronically quite different.

Complex **1b** is diamagnetic both in the solid state and in solution (EPR spectroscopy, Evans method,[13] ^{1}H and ^{31}P NMR spectroscopy, see the Supporting Information). The ^{31}P NMR spectrum of **1b** shows a resonance signal at $\delta = 134.4$ ppm, which is very different from the value observed for the free P_4 molecule ($\delta = -519$ ppm). It is noteworthy that ^{31}P NMR resonances reported for other compounds containing coordinated P_4 molecules usually appear at much higher fields ($\delta = -282$ to -497 ppm).[12a] The low-field shift of **1b** suggests P–P bond activation within the P_4 unit. However, most striking is the fact that the P_4 ligand is not reduced to a (formally) dianionic P_4 subunit by the two Ni^{I} centers (see below), in contrast to the result of the facile redox reaction of P_4 with $[(\eta^5\text{-}\mathrm{C}_5\mathrm{Me}_5)\mathrm{Ni}]$ fragments[1d] and low-valent main group metals.[4b] Compound **1a** is diamagnetic in the solid state, too. However, to our surprise and unlike $[\{(\eta^5\text{-}\mathrm{C}_5\mathrm{Me}_5)\mathrm{Ni}\}_2\mathrm{P}_4]$,[1d] dissolution of crystals of **1a** in hydrocarbons leads to a deep green solution which contains open-shell species as indicated by sharp, paramagnetically shifted resonance signals in the ^{1}H NMR spectra at room temperature (see the Supporting Information). The most unusual shifts for **1a** are observed for the γ-ring CH proton on the $\mathrm{C}_3\mathrm{N}_2\mathrm{Ni}$ rings and the terminal methyl protons as well as for the *para*-protons on the phenyl rings, which display signals at $\delta = -1.38$, 0.98, and 2.43 ppm, respectively. In addition, no resonance signal could be observed in the ^{31}P NMR spectrum because of excessive line broadening. Accordingly, the effective magnetic moment of **1a** in toluene determined by the Evans method[13] proved the presence of a paramagnetic species at room temperature, but the actual value of 0.93 μ_B represents only a paramagnetic fraction of about 29%, or, in other words, one spin $S=\frac{1}{2}$ per three to four molecules of **1a**. These observations are reminiscent of the dissociation of the complexes $[(L^{iPr}Ni)_2E_2]$ (E=Se and Te),[9c] which give rise to paramagnetic superchalcogenides $[L^{iPr}NiE_2]$. Therefore, we believe that a similar dissociation occurs when **1a** is dissolved in hydrocarbons, which leads to the paramagnetic species $[L^{iPr}NiP_4]$ (**2a**) and $[L^{iPr}Ni^I]$ (Scheme 3). In fact, the presence of the latter species in solutions is supported by high-resolution electrospray ionization mass spectrometry (HR ESI-MS; see the Supporting Information).

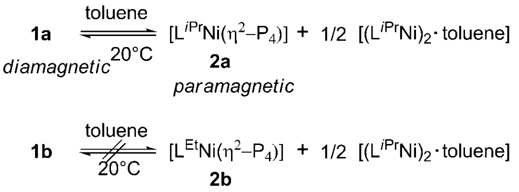

Scheme 3. Dissociation of **1a** to **2a** and $[(L^{iPr}Ni)_2{\cdot}toluene]$.

Additionally, X-band EPR measurements of **1a** in frozen toluene solution at 50 K confirmed the presence of a paramagnetic species with an $S=\frac{1}{2}$ ground state (Figure 2). The EPR spectrum, showing anisotropic Zeeman and hyperfine splitting, is centered at $g\approx 2.15$. A salient three-line pattern at the low-field edge indicates sizable hyperfine coupling with two equivalent nuclear spins of $I=\frac{1}{2}$ (giving rise to a triplet with a 1:2:1 intensity ratio), which we assign to the ^{31}P nuclei of two coordinated phosphorus atoms. Appreciable hyperfine interaction of two more ^{31}P nuclei can be inferred from the line triplet at the high-field edge of the spectrum, which shows less splitting. Accordingly, the EPR spectrum could be reasonably well simulated by adopting a set of rhombic g values (2.07, 2.11, 2.25) and hyperfine interaction with four phosphorus nuclei, grouped in two pairs with coupling constants $A_{1,2}=(-75, -40, -130)\times 10^{-4}\,cm^{-1}$ and $A_{3,4}=(-30, -30, -20)\times 10^{-4}\,cm^{-1}$. The assignment of spectral lines to particular g and A values is visualized by a hierarchical stick spectrum at the top of Figure 2.

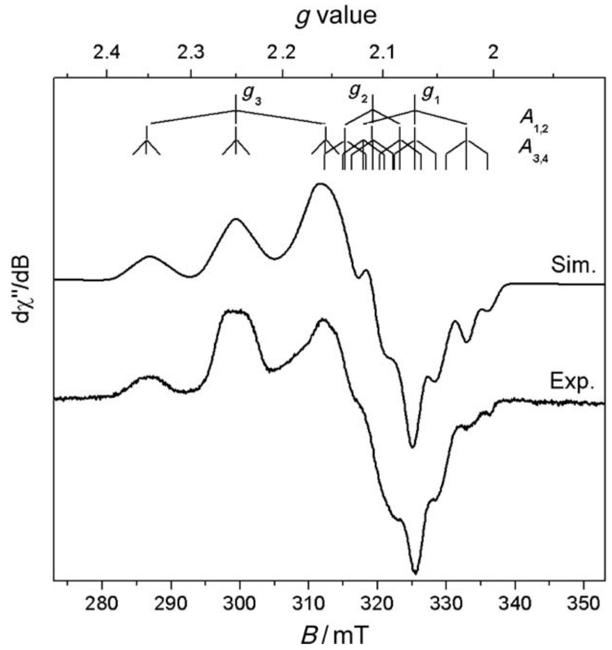

Figure 2. X-band EPR spectrum of **1a** in frozen toluene at 50 K. The top line (Sim.) is a powder simulation with anisotropic g and A values as mentioned in the text. The stick spectra at the top indicate the g and A splittings at the principal values of the respective matrices.

The large anisotropy of the g values indicates a metal-centered spin, that is the presence of nickel(I). The values actually resemble those of Ni^I complexes compiled by Saraev et al., including examples with β-diketiminate ligands.[14a] In addition, the relatively weak isotropic coupling constants for the ^{31}P nuclei, $A_{1,2,\,iso}=-82\times 10^{-4}\,cm^{-1}$ and $A_{3,4,\,iso}=-27\times 10^{-4}\,cm^{-1}$, preclude the presence of a phosphorus radical.[14b] Apparently, the paramagnetic species of dissolved **1a** is a monomeric nickel (I) complex, **2a**, in which the neutral P_4 ligand is bound in an η^2-fashion. This hypothesis is well supported by DFT calculations (see the Supporting Information), which even provide an optimized structure for **2a** (see Figure 3) that is found to be of the type **B** in Scheme 1. For this geometry, the calculations predict that 95% of the spin density is localized on the tetrahedral coordinated Ni atom (see Figure S5 in the Supporting Information) in agreement with the Ni^I assignment from the EPR data.

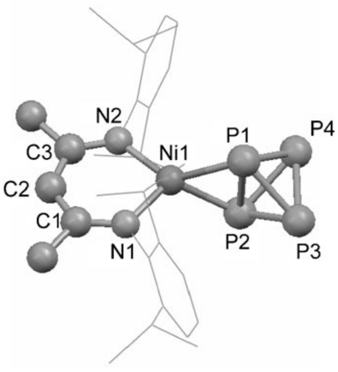

Figure 3. DFT-derived optimized molecular structure of **2a**.

Double-integration of the EPR spectrum and comparison with a Cu^{II} standard reveals a spin concentration of about 20% relative to the concentration of dissolved **1a**. This presumably reflects the concentration of **2a** at the freezing point of toluene, and compares well with the value of 29% found from the magnetic measurement (Evans method) at ambient temperature. Thus, the dissociation is temperature dependent, as expected. The fact that no second paramagnetic species is detected can be explained by dimerization of the $[L^{iPr}Ni^I]$ molecules released upon dissociation of **1a**, leading to the formation of the diamagnetic solvate $[(L^{iPr}Ni)_2\cdot$toluene$]$.[8]

Remarkably, DFT calculations also support a Ni^I description for the nickel atoms in **1a** and **1b**. Strong antiferromagnetic coupling between the Ni^I sites is mediated via superexchange through the bridging P_4 ligand (Figure 4).

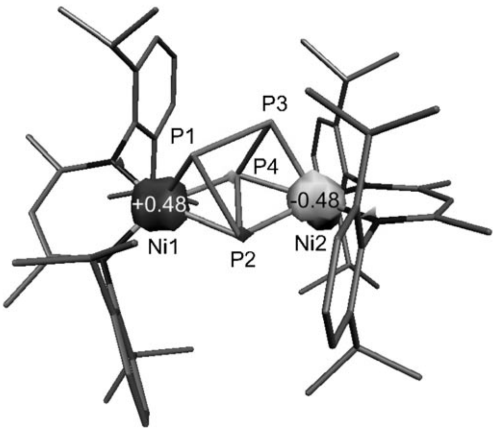

Figure 4. DFT-calculated spin density of diamagnetic **1a** from Mulliken population analysis of a B3LYP broken symmetry BS(1,1) calculation.

The differing behavior of **1a** and **1b** in solutions could only be rationalized by less steric congestion in **1b**. For a similar reason, the $[(L^{iPr}Ni)_2E_2]$ (E = S, Se, and Te) complexes behave differently in solutions.[9c] Remarkably, the calculated reaction energies for the dissociation of **1a** and **1b** to give **2a** and **2b**, respectively (Scheme 3), are predicted to be -6.1 and $+40.6\,kJ\,mol^{-1}$, respectively. Considering the additional formation of the corresponding $[(LNi^I)_2\cdot$toluene$]$ in the presence of toluene, the reaction energies are calculated to be -26.9 and $+0.6\,kJ\,mol^{-1}$ for **1a** and **1b**, respectively. Thus, the computations predict the correct trend for the dissociation. However, the reaction energies seem to be underestimated, which is possibly due to the neglect of solvation effects.

In summary, the unique nickel complexes **1a** and **1b**, which contain a η^3-coordinated P_4 ligand between two Ni^I atoms, were isolated from the reaction of ß-diketiminate Ni^I precursors with P_4. Remarkably, the activation occurs without P_4 reduction; that is, the complexes still contain Ni^I sites. While their solid-state structures are almost akin to each other, **1a** undergoes reversible dissociation in solutions, in contrast to **1b**, to give the paramagnetic η^2-coordinated P_4 Ni^I complex **2a** and $[(L^{iPr}Ni)_2\cdot$toluene$]$ by dimerization of $[L^{iPr}Ni^I]$, as suggested by the NMR, HR-MS, and EPR spectroscopic data as well as computational calculations.

Acknowledgements

Financial support from the Cluster of Excellence "Unifying Concepts in Catalysis" (EXC 314/1; administered by the TU Berlin and financed by the Deutsche Forschungsgemeinschaft) is gratefully acknowledged. We thank Dr. M. Schlangen (TU-Berlin) for HR-ESI mass spectra.

Keywords: bond activation · EPR spectroscopy · main group elements · phosphorus · diketiminate · superexchange

[1] a) M. P. Ehses, A. Romerosa, M. Peruzzini, *Top. Curr. Chem.* **2002**, *220*, 107; b) M. Peruzzini, R. R. Abdreimova, Y. Budnikova, A. Romerosa, O. J. Scherer, H. Sitzmann, *J. Organomet. Chem.* **2004**, *689*, 4319; c) M. Peruzzini, L. Gonsalvi, A. Romerosa, *Chem. Soc. Rev.* **2005**, *34*, 1038; d) O. J. Scherer, *Acc. Chem. Res.* **1999**, *32*, 751; and references therein; e) O. J. Scherer, J. Braun, P. Walther, G. Wolmershäuser, *Chem. Ber.* **1992**, *125*, 2661; f) M. Scheer, U. Becker, *Chem. Ber.* **1996**, *129*, 1307.

[2] A. P. Ginsberg, W. E. Lindsell, *J. Am. Chem. Soc.* **1971**, *93*, 2082.

[3] a) B. M. Cossairt, C. C. Cummins, *Angew. Chem.* **2008**, *120*, 8995; *Angew. Chem. Int. Ed.* **2008**, *47*, 8863; b) B. M. Cossairt, C. C. Cummins, *Angew. Chem.* **2008**, *120*, 175; *Angew. Chem. Int. Ed.* **2008**, *47*, 169; c) W. W. Seidel, O. T. Summerscales, B. O. Patrick, M. D. Fryzuk, *Angew. Chem.* **2009**, *121*, 121; *Angew. Chem. Int. Ed.* **2009**, *48*, 115.

[4] a) A. R. Fox, R. J. Wright, E. Rivard, P. P. Power, *Angew. Chem.* **2005**, *117*, 7907; *Angew. Chem. Int. Ed.* **2005**, *44*, 7729; b) Y. Peng, H. Fan, H. Zhu, H. W. Roesky, J. Magull, C. E. Hughes, *Angew. Chem.* **2004**, *116*, 3525; *Angew. Chem. Int. Ed.* **2004**, *43*, 3443.

[5] J. M. Lynam, *Angew. Chem.* **2008**, *120*, 843; *Angew. Chem. Int. Ed.* **2008**, *47*, 831.

[6] a) J. D. Masuda, W. W. Schoeller, B. Donnadieu, G. Bertrand, *J. Am. Chem. Soc.* **2007**, *129*, 14180; b) J. D. Masuda, W. W. Schoeller, B. Donnadieu, G. Bertrand, *Angew. Chem.* **2007**, *119*, 7182; *Angew. Chem. Int. Ed.* **2007**, *46*, 7052; c) O. Back, G. Kuchenbeiser, B. Donnadieu, G. Bertrand, *Angew. Chem.* **2009**, *121*, 5638; *Angew. Chem. Int. Ed.* **2009**, *48*, 5530.

[7] a) M. Driess, S. Yao, M. Brym, C. van Wüllen, D. Lenz, *J. Am. Chem. Soc.* **2006**, *128*, 9628; b) Y. Xiong, S. Yao, M. Brym, M. Driess, *Angew. Chem.* **2007**, *119*, 4595; *Angew. Chem. Int. Ed.* **2007**, *46*, 4511.

[8] D. Bai, P. Wei, D. W. Stephan, *Organometallics* **2005**, *24*, 5901.

[9] a) S. Yao, E. Bill, C. Milsmann, K. Wieghardt, M. Driess, *Angew. Chem.* **2008**, *120*, 7218; *Angew. Chem. Int. Ed.* **2008**, *47*, 7110; b) S. Yao, C. Milsmann, E. Bill, K. Wieghardt, M. Driess, *J. Am. Chem. Soc.* **2008**, *130*, 13536; c) S. Yao, Y. Xiong, X. Zhang, M. Schlangen, H. Schwarz, C. Milsmann, M. Driess, *Angew. Chem.* **2009**, *121*, 4621; *Angew. Chem. Int. Ed.* **2009**, *48*, 4551; d) S. Pfirrmann, C. Limberg, C. Herwig, R. Stößer, B. Ziemer, *Angew. Chem. Int. Ed.* **2009**, *48*, 3357; e) D. J. Mindiola, *Angew. Chem.* **2009**, *121*, 6314.

[10] S. Pfirrmann, C. Limberg, B. Ziemer, *Dalton Trans.* **2008**, 6689.

[11] Y. Xiong, S. Yao, M. Driess, unpublished results.

[12] See, for example: a) I. Krossing, *J. Am. Chem. Soc.* **2001**, *123*, 4603; b) A. P. Ginsberg, W. F. Lindsell, K. J. McCullough, C. R. Sprinkle, A. J. Welch, *J. Am. Chem. Soc.* **1986**, *108*, 403; c) O. J. Scherer, M. Swarowsky, G. Wolmerschäuser, *Organometallics* **1989**, *8*, 841.

[13] a) D. F. Evans, *J. Chem. Soc.* **1959**, 2003; b) T. Ayers, R. Turk, C. Lane, J. Goins, D. Jameson, S. J. Slattery, *Inorg. Chim. Acta* **2004**, *357*, 202.

[14] a) V. V. Saraev, P. B. Kraikivskii, I. Svoboda, A. S. Kuzakov, R. F. Jordan, *J. Phys. Chem. A* **2008**, *112*, 12449; b) B. F. M. De Waal, O. M. Aagaard, R. A. J. Janssen, *J. Am. Chem. Soc.* **1991**, *113*, 9471.

Received: October 13, 2009